Lipid Membrane Expansion and Micelle Formation by Polymer-Grafted Lipids: Scaling with Polymer Length Studied by Spin-Label Electron Spin Resonance

Giuseppina Montesano,* Rosa Bartucci,* Salvatore Belsito,* Derek Marsh,[†] and Luigi Sportelli*

*Dipartimento di Fisica and Unità INFM, Università della Calabria, I-87036 Arcavacata di Rende (CS) Italy, and [†]Max-Planck-Institut fur Biophysikalische Chemie, Abteilung Spektroskopie, 37070 Göttingen, Germany

ABSTRACT   Spin-label electron spin resonance (ESR) spectroscopy and auxiliary optical density measurements are used to study lipid dispersions of N-poly(ethylene glycol)-dipalmitoyl phosphatidylethanolamine (PEG:5000-DPPE) mixed with di-palmitoyl phosphatidylcholine (DPPC). PEG:5000-DPPE bears a large hydrophilic polymer headgroup (with ~114 oxyethylene monomers) and is commonly used for steric stabilization of liposomes used in drug delivery. Comparison is made with results from mixtures of DPPC with polymer lipids bearing shorter headgroups (~45 and 8 oxyethylene monomers). ESR spectra of phosphatidylcholine spin-labeled on the 5-C atom position of the sn-2 chain are shown to reflect the area expansion of the lipid membranes by the lateral pressure exerted in the polymer brush, in a way that is consistent with theory. The lipid chain packing density at the onset of micelle formation is the same for all three PEG-lipids, although the mole fraction at which this occurs differs greatly. The mole fraction at onset scales inversely with the size of the polymer headgroup, where the experimental exponent of 0.7 is close to theoretical predictions (viz. 0.55–0.6). The mole fraction of PEG-lipid at completion of micelle formation is more weakly dependent on polymer size, which conforms with theoretical predictions. At high mole fractions of PEG:5000-DPPE the dependence of lipid packing density on mole fraction is multiphasic, which differs qualitatively from the monotonic decrease in packing density found with the shorter polymer lipids. Lipid spin-label ESR is an experimental tool that complements theoretical analysis using polymer models combined with the lipid equation of state.

INTRODUCTION

Supramolecular structures composed of amphiphilic molecules (liposomes, nanoparticles, etc.) are currently used widely in several biotechnological and biomedical areas (Lasic, 1993; Lasic and Needham, 1995). Admixture with common diacyl lipids of phosphatidylethanolamines N-derivatized in the headgroup with bulky hydrophilic polymers such as poly(ethylene glycol) are now used routinely for steric stabilization in vivo of liposomal drug carriers and delivery systems (see, e.g., Blume and Cevc, 1990; Lasic, 1993; Lasic and Martin, 1995). These liposome formulations show prolonged lifetimes in the circulation, relative to conventional phospholipid vesicles, because of the steric barrier imposed at the liposome surface by the grafted polymer chains (Klibanov et al., 1990; Allen et al., 1991; Papahadjopoulos et al., 1991; Lasic et al., 1991; Blume and Cevc, 1993; Torchilin et al., 1994).

In the present work we study lipid dispersions of zwitterionic dipalmitoyl phosphatidylcholine mixed with a poly-(ethylene glycol) lipid (PEG-lipid) of high molecular weight (average degree of polymerization 114 oxyethylene units) by using lipid spin-label electron spin resonance (ESR) spectroscopy. This PEG-grafted lipid is one of those most frequently used for steric stabilization of phosphatidylcho-

line liposomes (e.g., Lasic, 1993; Lasic and Martin, 1995). The Flory radius of a PEG-polymer of this size is $R_F \approx 6.7$ nm, so that at practically all contents of polymer lipid one is dealing with the brush regime of surface coverage by the polymer. Previously we have demonstrated that lipid spin-label ESR spectroscopy can be used, combined with the Gibbs phase rule, to quantitate micelle formation induced by polymer lipids. This was done with PEG-lipids of lower molecular weight that have average degrees of polymerization 8 and 45 (Belsito et al., 2000). Here, together with additional measurements on the shorter PEG-lipids, we concentrate on the expansion of the lipid surface that is induced by the lateral pressure in the polymer brush of the grafted lipids. Extension to the long polymer lipid (PEG:5000-DPPE) now permits analysis of the scaling properties of the micellization process with length of the grafted polymer.

Strong emphasis is placed on comparison of the experimental results with theoretical predictions. The latter use models from polymer physics (Hristova and Needham, 1994, 1995), combined with the equation of state for the lipids (Marsh, 1996) that characterizes the effects of lateral pressure in lipid aggregates. The extent of agreement between theory and experiment is extremely satisfactory.

MATERIALS AND METHODS

Materials

Synthetic 1,2-dipalmitoyl-sn-glycero-3-phosphatidylcholine (DPPC) was from Sigma (St. Louis, MO). High-purity (>99%) poly(ethylene glycol)-lipids (PEG-lipids), 1,2-dipalmitoyl-sn-glycero-3-phosphatidylethanolamine-N-poly(ethylene glycol), with average polymer molecular weights

of 5000 (PEG:5000-DPPE), 2000 (PEG:2000-DPPE), and 350 (PEG:350-DPPE), and spin-labeled lipids 1-palmitoyl-2-(*n*-doxyl stearoyl)-*sn*-glycero-3-phosphocholine (*n* = 5, 16; 5-, 16-PCSL) were obtained from Avanti Polar Lipids (Birmingham, AL). Poly(ethylene glycol)methyl ether with average molecular weight 5000 (PEG:5000) was from Aldrich (Steinheim, Germany). Reagent grade salts for the 10 mM phosphate buffer solution (PBS) at pH 7.5 were from Merck (Darmstadt, Germany). All materials were used as purchased with no further purification. Distilled water was used throughout.

ESR measurements

Hand-shaken lipid dispersions for ESR measurements were prepared by first dissolving the required amounts of DPPC and PEG-DPPE lipid in chloroform, together with 1% by weight of either 5- or 16-PCSL spin label. The solvent was evaporated in a stream of nitrogen gas and the lipid film was then kept under vacuum overnight. Finally, the dried lipids were fully hydrated with PBS at pH 7.5 at final lipid concentration of 25 mM by heating at 60°C and periodically vortexing for 40 min. The homogeneous lipid dispersions were sealed in 1-mm (I.D.) 100-μl glass capillaries and stored overnight at 10°C before the ESR measurements. ESR spectra were recorded with a Bruker (Karlsruhe, Germany) ER 200D-SRC spectrometer operating at 9 GHz that was equipped with an ER 4111 VT variable temperature control unit (accuracy ±0.5°C) and an ESP 1600 data system for spectral acquisition and processing. The sample capillary was inserted in a standard 4-mm I.D. quartz ESR tube that contained light silicone oil for thermal stability, and was centered in the rectangular TE_{102} ESR cavity resonator (ER 4201, Bruker). Conventional, first harmonic in-phase, absorption ESR signals were recorded at 10 mW microwave power, with field modulation of amplitude 1 G_{p-p} at 100 kHz frequency for the phase-sensitive detection.

Single-component ESR spectra of 5-PCSL were analyzed by measuring the outer hyperfine splitting, $2A_{max}$, or the difference between the outer and inner hyperfine splittings $\Delta A = 2(A_{max} - A_{min})$, at low temperature (10°C) and at high temperature (50°C), respectively. In the fluid phase, the spectra of 16-PCSL were, instead, analyzed by measuring the apparent linewidth of the high-field hyperfine manifold. These parameters reflect the segmental motion of hydrocarbon lipid chains (Marsh, 1981, 1989). At certain temperatures in the gel phase, the conventional ESR spectra of 5- and 16-PCSL show two distinct spectral components. These were resolved by performing spectral subtractions as described in Marsh (1982).

Spectrophotometric measurements

DPPC/PEG:5000-DPPE dispersions were prepared for spectrophotometric measurements at a final lipid concentration of 1 mg/ml, as described above but without addition of spin label. The lipid suspensions were transferred to 3-ml quartz cells of 1-cm optical path and incubated overnight at 10°C before measuring.

Optical density measurements were made at 400 nm (OD_{400}) with a Jasco 7850 spectrophotometer that was equipped with a Peltier thermostatted cell holder model EHC-441 and a temperature programmer model TPU-436 (accuracy ± 0.1°C). A heating rate of 1°C/min was used. Data acquisition and processing were carried out with the spectrophotometer's built-in microcomputer. Spin-label ESR and spectrophotometric data are single measurements, but the experiments have been repeated to test the reproducibility of the results.

RESULTS

Spectrophotometry

The optical density at 400 nm for mixtures of DPPC with PEG:5000-DPPE at various molar ratios is given as a func-

tion of temperature in Fig. 1. The pretransition and the main transitions are clearly seen at temperatures of $T_p \cong 32.0°C$ and $T_m \cong 41.5°C$, respectively, in the thermal profile of the DPPC aqueous dispersion (Fig. 1 and Table 1). Addition of the PEG-lipid affects the characteristics of both thermal transitions. Indeed, T_p increases progressively to ~35.5°C at 30 mol % PEG:5000-DPPE, the amplitude of the transition decreases, its width increases, and the pretransition finally disappears at PEG:5000-DPPE contents >30 mol % (Fig. 1 and Table 1). The main transition temperature first decreases a little with the addition of the lowest content of the PEG-lipid, then remains approximately constant up to 30 mol % and finally drops to 38.4°C at 40 mol %, and to
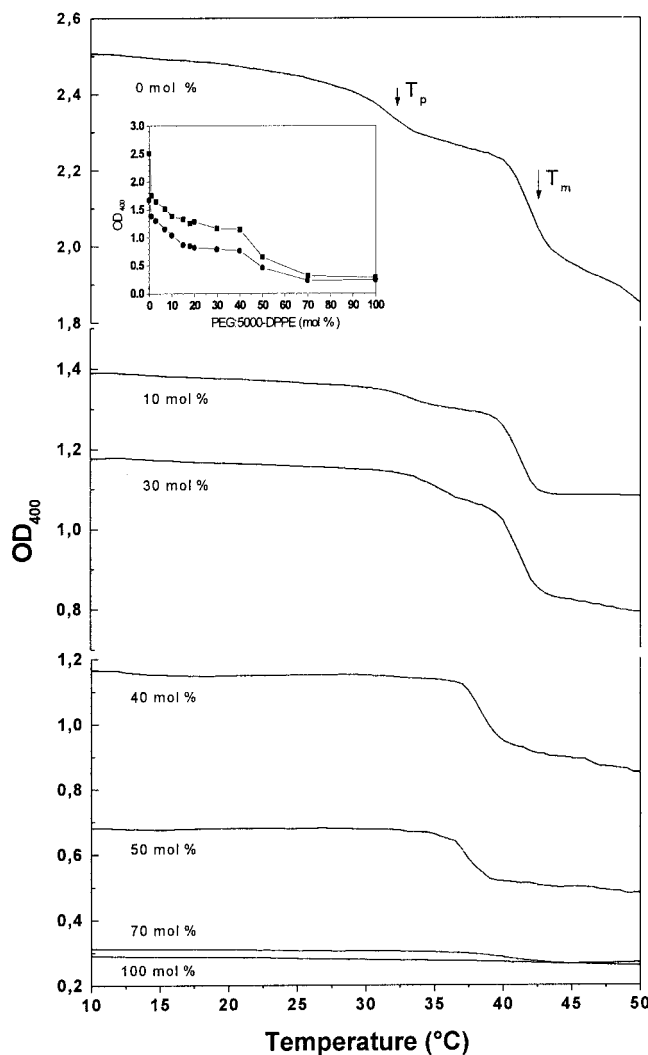

FIGURE 1 Temperature-dependence of the optical density at 400 nm for aqueous dispersions of DPPC/PEG:5000-DPPE mixtures. The arrows indicate the temperatures at which the pretransition and the main transition are detected, respectively, in DPPC dispersions. The inset shows the dependence of OD_{400} on PEG:5000-DPPE lipid content in aqueous dispersions of DPPC/PEG:5000-DPPE mixtures at 10°C (*squares*) and 50°C (*circles*). The errors are smaller than the symbols.

TABLE 1 Temperatures of pre (T_p) and main phase transitions (T_m) in aqueous mixtures of DPPC/PEG:5000-DPPE at different mole fractions, as determined by spectrophotometry

PEG:5000-DPPE (mol %)	T_p (°C)*	T_m (°C)*
0	32.0	41.5
1	33.5	41.0
3	33.6	41.0
7	33.8	41.2
10	34.7	41.0
15	34.8	41.0
20	35.2	41.0
30	35.5	41.0
40	—	38.4
50	—	37.5
70	—	—
100	—	—

*The error in T_p and T_m is 0.1°C.

37.5°C at 50 mol %. Beyond this concentration of polymer-lipid, the main chain-melting transition of the dispersions is no longer detected, i.e., the optical density remains approximately constant throughout the whole temperature range (Fig. 1 and Table 1). A further notable feature of Fig. 1 is that progressive addition of polymer lipid in the DPPC host lipid matrix markedly decreases the optical turbidity at any fixed temperature. As is shown in the inset to Fig. 1 corresponding to measurements at 10°C, the value of OD_{400} decreases rapidly from 2.5 for dispersions of DPPC alone to 1.7 at 3 mol % of PEG:5000-DPPE. It then decreases more slowly to 1.25 at 20 mol % PEG:5000-DPPE, maintains this value up to 40 mol %, and finally drops close to zero for 70 mol % onward. A very similar dependence on composition is observed at 50°C, except that the optical densities are

somewhat lower than the corresponding ones at 10°C. Moreover, the difference between the optical densities at low and high temperature decreases on increasing the PEG:5000-DPPE content, and becomes approximately zero at 70 mol % of the polymer lipid.

ESR of 5-position spin-labeled phosphatidylcholine at low temperature

ESR spectra of 5-PCSL recorded at a temperature of 10°C that correspond to the gel phase of DPPC dispersions (Mabrey and Sturtevant, 1976) are given in Fig. 2 *A* for various DPPC/PEG:5000-DPPE mixtures. Up to 50 mol %, a progressive decrease in splitting ($2A_{max}$) between the two outermost hyperfine peaks is seen on increasing the content of polymer lipid in the mixed-lipid dispersions. This decrease in spectral splitting corresponds to an increase in mobility of the spin-labeled lipid chains. Because the measurements are performed at the same temperature, and because the chain composition of the polymer lipid is identical to that of the nonpolymer lipid, this increase in chain mobility must correspond to a decrease in packing density of the lipid chains as the content of polymer lipid in the dispersions is increased (see also, e.g., Cevc and Marsh, 1987). Beyond 50 mol % of the PEG-lipid, the spectral anisotropy shows a surprising but highly reproducible behavior. Indeed, it first increases up to contents of 70 mol % and then again decreases approaching that characteristic for micelles of the polymer lipid alone.

The dependence of the outer hyperfine splitting, $2A_{max}$, at 10°C on content of polymer lipid in the DPPC/PEG:5000-DPPE mixed lipid dispersions is given in Fig. 3 *A*. Corresponding data for DPPC/PEG:2000-DPPE and DPPC/PEG:
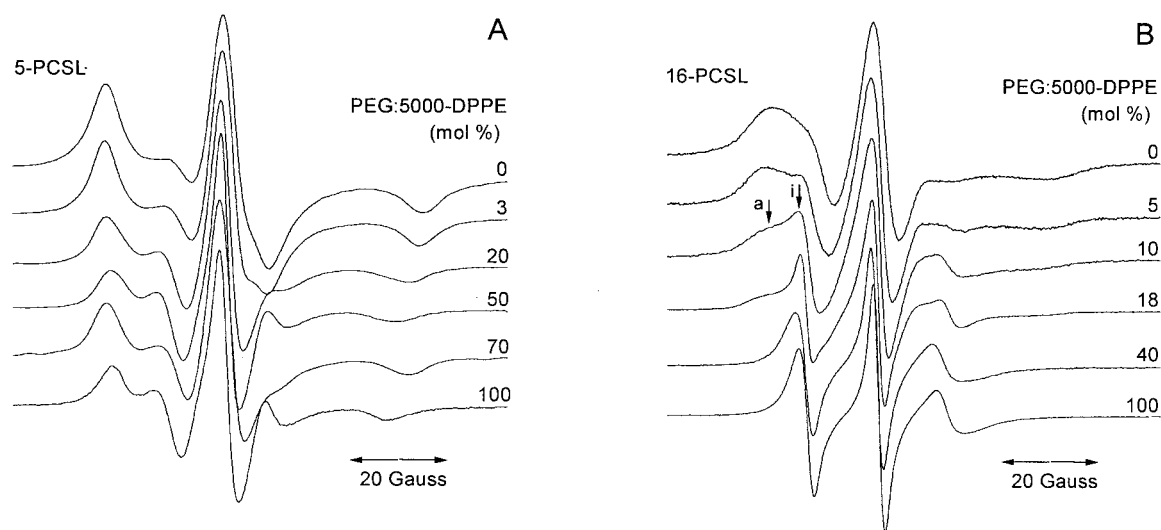

FIGURE 2 Conventional ESR spectra at 10°C of (*A*) 5-PCSL and (*B*) 16-PCSL in aqueous dispersions of DPPC/PEG:5000-DPPE mixtures at the mole fractions indicated on the figure. Total scan width = 100 G.
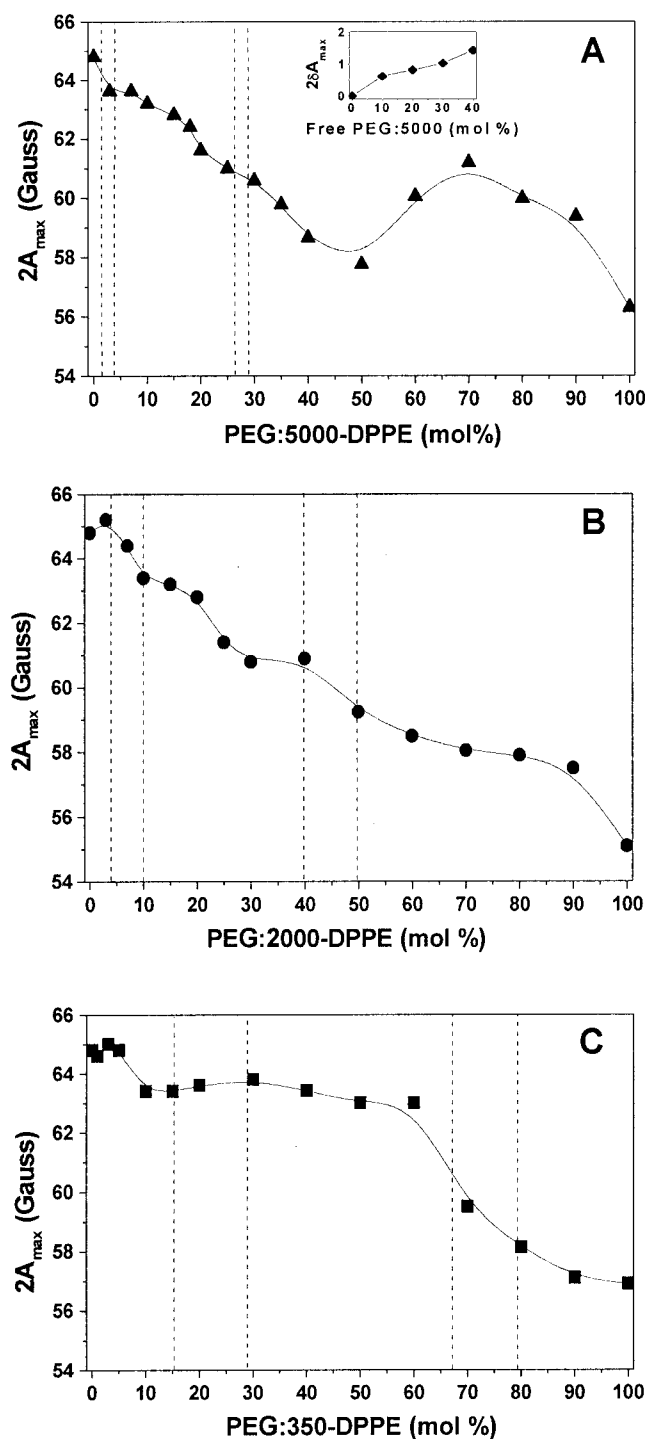
FIGURE 3 Dependence of the outer hyperfine splitting, $2A_{max}$, at 10°C of the 5-PCSL spin label on PEG-DPPE lipid content in aqueous dispersions of (A) DPPC/PEG:5000-DPPE mixtures, (B) DPPC/PEG:2000-DPPE mixtures, and (C) DPPC/PEG:350-DPPE mixtures. The errors are smaller than the symbols. *Inset*: change ($2\delta A_{max}$) in the value of $2A_{max}$ for 5-PCSL in DPPC/PGE:5000-DPPE (1:1 mol/mol) dispersions on adding increasing concentrations of free PEG:5000 polymer to the bulk suspending medium. Fine dashed vertical lines represent the ranges of uncertainty in PEG-lipid content at the onset and completion of the bilayer-micelle transition, obtained from the least-squares fits in Fig. 4.

350-DPPE dispersions are given in Fig. 3, *B* and *C,* respectively. Both features in common and differences dependent on the size of the lipid polymer-headgroup are evident from comparison of the three parts of Fig. 3. It should be noted that, at 10°C, the samples are well below the chain-melting temperature of the bilayer component of the mixtures that is recorded by the sharp decrease in optical density evident in Fig. 1 (see also Table 1). Confirmation of this comes from the relatively high values of $2A_{max}$ for 5-PCSL that are analyzed below.

Low contents of PEG-lipid

For DPPC/PEG:5000-DPPE dispersions there is a rapid, small decrease in $2A_{max}$ between 0 and 3 mol % of PEG: 5000-DPPE. After an initial short quasi-constant region in the mushroom regime, a similar drop in $2A_{max}$ is seen for both DPPC/PEG:2000 and DPPC/PEG:350 mixed lipid dispersions. The content of polymer lipid at which this decrease is achieved increases, however, with decreasing length of the polymer chain. It occurs at mole fractions of ~10 and 15 mol % for PEG:2000-DPPE and PEG:350-DPPE, respectively. It will be seen later that these different polymer-lipid contents correspond approximately with those at which micelle formation is initiated. A very significant feature is that the initial decrease in $2A_{max}$, and hence in lipid packing density, is the same for all three polymer lipids. It corresponds to a reduction from the value in DPPC alone to a common value of $2A_{max} \sim$ 63.5 G in all three cases. This point will be returned to later, in the discussion of the scaling properties of the onset of micelle formation with increasing polymer length.

Intermediate contents of PEG-lipid

A striking aspect of the results in Fig. 3 *C* is that, beyond the initial decrease, the values of $2A_{max}$ for 5-PCSL remain approximately constant (at ~63.5 G) in DPPC/PEG:350-DPPE dispersions up to total mole fractions of 60 mol % of the polymer lipid. As will be seen later, micelle formation is complete at mole fractions of PEG:350-DPPE just beyond this value, at ~70 mol % (see also Belsito et al., 2000). The high values of $2A_{max}$ in this constant region indicate that these spectral splittings correspond to the lamellar gel-phase component in the mixed lipid dispersions. The values of $2A_{max}$ for micelles are considerably smaller (~57 G) at the same temperature, as is seen for the purely micellar samples with 80 mol % PEG:350-DPPE and above (see Fig. 3 *C*). The values in the plateau region are also far greater than the value of $2A_{max}$ for lamellar DPPC in the fluid phase, which is maximally 47 G at a temperature just above the chain-melting transition. These observations are consistent with the predictions of the Gibbs phase rule for a macroscopic separation between the lamellar and micellar phases. Throughout the region of bilayer-micelle conversion, the

composition of the coexisting phases remains constant, according to the phase rule (cf. Belsito et al., 2000). Therefore it is expected that the values of $2A_{max}$ for the two phases should remain constant, independent of the total lipid composition, throughout the coexistence region. This is exactly what is observed in Fig. 3 C for the lamellar component of the DPPC/PEG:350-DPPE mixtures.

The regions of bilayer-micelle coexistence for DPPC/PEG:2000-DPPE and DPPC/PEG:5000-DPPE mixtures become progressively narrower with increasing polymer length, as compared with the DPPC/PEG:350-DPPE mixtures (see below). A well-developed constant region of $2A_{max}$ for 5-PCSL is not seen in these former two mixtures (Fig. 3, A and B). Instead, a moderate decrease in $2A_{max}$ is found during the region of bilayer-micelle conversion. The value at the end of the transition region, ~61 G for both PEG:5000 and PEG:2000, is still that characteristic of a lamellar gel phase and not that typical of micelles. Because the results with PEG:350-DPPE are consistent with the phase rule, one would expect this also to be true for other polymer lipids, on purely thermodynamic grounds. (Note that, in excess water, we are dealing with a two-component system and therefore, according to the phase rule, only two phases may coexist over a range of compositions.) Hence the decrease in $2A_{max}$ of 5-PCSL in the transition regions with PEG:5000-DPPE and PEG:2000-DPPE is unlikely to be caused by changing composition of the lamellar phase. Most probably, it arises from a decrease in particle size of the lamellar structures as progressively more DPPC is incorporated into micelles with increasing concentration of polymer lipid. Possible supporting evidence for this suggestion comes from the comparative efficiencies with which the polymer lipids of different length reduce the optical density of the mixed lipid dispersions over this composition range (compare Fig. 1 with Fig. 1 of Belsito et al., 2000).

High contents of PEG-lipid

A systematic progression in the behavior of $2A_{max}$ with increasing polymer headgroup size is seen by comparing Fig. 3, A–C in the region of polymer-lipid contents corresponding to the micellar regime in each case. For PEG:350-DPPE, $2A_{max}$ monotonically approaches the value for micelles of the polymer lipid alone (see Fig. 3 C). For PEG:2000-DPPE, $2A_{max}$ tends instead to a plateau level as the polymer lipid content increases, with a rate of decrease similar to that for PEG:350-DPPE. The plateau level of $2A_{max}$ is greater than the value for micelles of PEG:2000-DPPE alone, which is only achieved at the highest polymer-lipid contents (see Fig. 3 B). For PEG:5000-DPPE, the trend in $2A_{max}$ is that, after decreasing up to polymer-lipid contents of 50 mol %, the values then *increase* up to contents of 70 mol % of polymer lipid. Beyond 70 mol %, the values of $2A_{max}$ then again decrease (see Fig. 3 A). Comparison of Fig. 3, A and B in the region of high polymer-lipid contents

suggests that the plateau behavior of $2A_{max}$ for PEG:2000-DPPE represents an attenuated version of the multiphasic behavior with PEG:5000-DPPE.

One possible mechanism for the "anomalous" increase in $2A_{max}$ with lipid dispersions containing PEG:5000-DPPE is indicated by the results presented in the inset to Fig. 3 A. Adding free PEG:5000 polymer to a dispersion of DPPC/PEG:5000-DPPE (1:1 mol/mol) results in a progressive increase in $2A_{max}$ with increasing concentration of the free polymer. At relatively high levels of grafting, the free polymer is unlikely to appreciably penetrate the dense polymer brush at the lipid surface. Therefore, the increase in $2A_{max}$ most probably is caused by a partial dehydration of the lipid surface that results from the well-known effects of the free PEG:5000 osmoticant on water activity. A similar effect is thus possible from the high surface density of PEG that is presented by the "endogenous" grafted polymer and indeed has been demonstrated at relatively low concentrations of PEG-lipid (Tirosh et al., 1998). Note, however, that the surface-anchored polymer must be more effective because the increase from 50 to 70 mol % PEG:5000-DPPE corresponds to an effective increase in bulk concentration by ~8 mol %. The highest osmoticant effect is contributed by the polymer lipid with the largest number of PEG monomers, i.e., PEG:5000-DPPE. For the PEG-lipids of lower molecular masses, the surface expansion resulting from the lateral pressure in the polymer brush outweighs the effects of surface hydration and no net increase in $2A_{max}$ is observed. A further possible mechanism for the increase in $2A_{max}$ with long grafted polymers will be presented in the Discussion.

ESR of 16-position spin-labeled phosphatidylcholine at low temperature

The ESR spectra of 16-PCSL at 10°C in dispersions of DPPC/PEG:5000-DPPE at different molar ratios are given in Fig. 2 B. The spectrum of 16-PCSL in dispersions of DPPC alone shows a lower degree of anisotropy and a considerable motional broadening relative to that of the 5-PCSL positional isomer (Fig. 2 A). This is expected for a noninterdigitated phospholipid lamellar gel phase (Bartucci et al., 1993). At the other extreme, the spectrum at 10°C of 16-PCSL in dispersions of the PEG:5000-DPPE polymer lipid alone is a near-isotropic triplet with differentially broadened ^{14}N hyperfine manifolds. This type of spectrum for 16-PCSL is characteristic of a more fluid environment that must correspond to polymer-lipid micelles. Addition of PEG:5000-lipid up to 5 mol % in the host lipid matrix of DPPC causes a restriction in motion of the spin-label lipid chains that is seen as an increase in the outer spectral hyperfine splitting. The spectra, in this range of polymer-lipid content, remain characteristic of a predominantly lamellar phospholipid gel phase. When the concentration of polymer-lipid is increased further, however, the ESR spec-

tra of 16-PCSL consist of a superposition of two spectral components. One component (designated *a* in Fig. 2 *B*), with larger outer hyperfine splitting, corresponds to spin-labeled lipids in a lamellar gel-phase environment that is characteristic of the mixtures with low content of PEG-lipid. The second, sharper spectral component (designated *i* in Fig. 2 *B*), corresponds to the quasi-isotropic environment of the micellar phase that is formed by the polymer-lipid alone at this temperature. (Note again that the cooperative chain melting of the gel-phase component that is seen in Fig. 1 occurs at a much higher temperature.) The relative proportion of the micelle-like component increases with increasing content of the PEG:5000-lipid over the range ∼7–30 mol %. For concentrations of polymer-lipid beyond this range, the spectra consist of a single component with lineshapes that resemble those of the spin label in PEG:5000-DPPE micelles alone.

Quantitation of lamellar and micellar components

The relative proportions of the 16-PCSL phosphatidylcholine spin label in the lamellar and micellar phases in the coexistence region can be determined by spectral subtraction and double integration of the two-component spectra, such as those shown in Fig. 2 *B* (see, e.g., Marsh, 1982). The results obtained from the single-component subtraction endpoints are given in terms of the fraction, f_{PC}(micelle), of 16-PCSL in micelles by the solid circles in Fig. 4. The coexistence of lamellar and micellar phases is also seen clearly in the two-component spectra of 5-PCSL in mixtures of DPPC and PEG:5000-DPPE obtained at temperatures higher than 10°C (spectra not shown). The results of subtractions with these spectra from the 5-PCSL phosphatidylcholine spin label at 30°C are given by the solid triangles in Fig. 4. To within experimental error, the results with 5-PCSL at higher temperatures are consistent with those of 16-PCSL at 10°C. As in our previous work (Belsito et al., 2000) and shown to be consistent with the phase rule, the portion of the spin-labeled lipid that gives rise to the spectral component characteristic of cooperative gel-lipid chain immobilization is assigned to the lamellar phase. The more isotropic spectral component in which the chains are more mobile and do not support such highly cooperative chain packing are assigned to micelles. The shape and size of the lipid aggregates may vary somewhat with composition, however, within an individual phase (Fig. 1, *inset*).

The heavy solid line in Fig. 4 is a nonlinear least-squares fit to the data from DPPC/PEG:5000-DPPE dispersions by using the dependence of the fraction of phosphatidylcholine in the micellar phase on total mole fraction of polymer lipid that is predicted by the Gibbs phase rule. According to the latter, the fraction, f_{tot}(micelle), of the total lipid (i.e., PC + PEG-lipid) that is converted to micelles is given by the lever
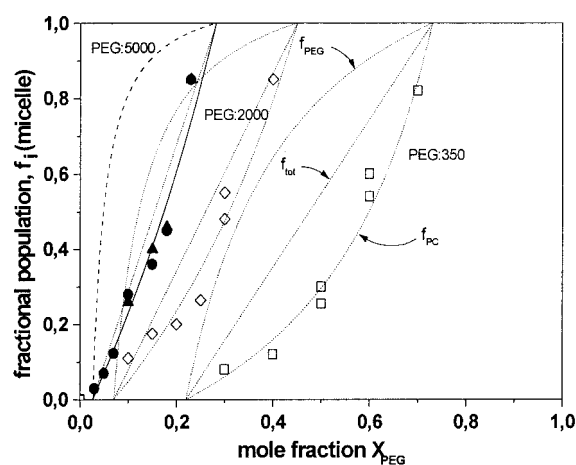

FIGURE 4 Fraction, f_{PC}(micelle), of the more fluid 16-PCSL component (*solid circles*) in the ESR spectra of aqueous dispersions of DPPC/PEG:5000-DPPE mixtures as a function of the PEG-lipid content, X_{PEG}, obtained from spectral subtractions at 10°C. Data from 5-PCSL at 30°C are given by the solid triangles. The heavy solid line is a nonlinear least-squares fit with Eqs. 1 and 2 for f_{PC} over the transition range. The heavy dotted and dashed lines are the degree of conversion to micelles of the total lipid (i.e., f_{tot}) and of the PEG-lipid component (i.e., f_{PEG}), respectively, calculated from Eqs. 1 and 3 by using the parameters obtained from the fit to the data with spin-labeled PC. Corresponding data for micellization of DPPC by admixture of PEG:2000-DPPE (*open diamonds*) or PEG:350-DPPE (*open squares*) are from Belsito et al. (2000), with the fitted and calculated values of f given by light dotted lines.

rule (Belsito et al., 2000):

$$f_{tot}(\text{micelle}) = \frac{X_{PEG} - X_{PEG}^{on}}{X_{PEG}^{end} - X_{PEG}^{on}} \quad (1)$$

where X_{PEG} is the total mole fraction of polymer lipid, and X_{PEG}^{on}, X_{PEG}^{end} are the values of X_{PEG} at the onset and completion, respectively, of the bilayer-micelle transition. The fraction, f_{PC}(micelle), of the phosphatidylcholine lipid component that is present in micelles is then related to the values of f_{tot}(micelle) by Belsito et al. (2000):

$$f_{PC}(\text{micelle}) = \frac{1 - X_{PEG}^{end}}{1 - X_{PEG}} f_{tot}(\text{micelle}) \quad (2)$$

Combination of Eqs. 1 and 2 then provides the function needed to fit the data from the PCSL phosphatidylcholine spin labels. It is seen from Fig. 4 that the phase rule provides an adequate description of micelle formation in the DPPC/PEG:5000-DPPE dispersions. The values of the fitting parameters are $X_{PEG}^{on} = 0.03 \pm 0.01$ and $X_{PEG}^{end} = 0.28 \pm 0.01$. These values can then be used to predict the fraction of the total lipid in the DPPC/PEG:5000-DPPE dispersions that is in the micellar form, by using Eq. 1. This is given by the heavy dotted line in Fig. 4. Correspondingly, the fraction of PEG-lipid, f_{PEG}(micelle), that is present as micelles is pre-

dicted from the phase rule to be:

$$f_{PEG}(\text{micelle}) = \frac{X_{PEG}^{end}}{X_{PEG}} f_{tot}(\text{micelle}) \quad (3)$$

This dependence on the total mole fraction of PEG:5000-DPPE in the mixed lipid dispersions is given by the heavy dashed line in Fig. 4.

For comparison, the corresponding data obtained from DPPC/PEG:2000-DPPE (*open diamonds*) and DPPC/PEG:350-DPPE (*open squares*) mixed lipid dispersions are also included in Fig. 4. In this case, the fitted and associated calculated dependences on mole fraction of PEG-lipid are given by light dotted lines. A progressive decrease in the PEG-lipid content at which conversion to micelles first occurs, and also in the width of the bilayer-micelle coexistence region, is found with increasing size of the polymer-lipid headgroup. The observed scaling with polymer length will be treated quantitatively later, in the Discussion section.

It should be noted that the above analysis assumes that the distribution of spin-labeled PC follows that of the unlabeled PC component in the mixtures with polymer lipid. Justification for this assumption lies not only in the agreement obtained with two quite different positions of spin labeling, 5-PCSL and 16-PCSL (see also Belsito et al., 2000), but also in the form of the dependence of f_{PC}(micelles) on PEG lipid content deduced from the spin-label measurements that is given in Fig. 4. The fractional population of spin-labeled PC that is in micelles lies below the line joining the points of onset and completion of micellization (i.e., of f_{tot}) and curves downward with increasing concentration of PEG-lipid in the mixture. This is opposite to the behavior predicted if spin-labeled PC preferentially partitioned into the micelles. Then the values of f_{PC}(micelle) deduced from spin-labeled PC would lie above the f_{tot}-line and curve upward with increasing PEG-lipid content. Evidently, it is the bulky polymer headgroup of the PEG-lipid that not only drives micelle formation but also controls the preferential partitioning of the PEG-lipid into the micelles. Compared with this, the spin label group is a rather minor perturbation of the lipid structure.

ESR of 5- and 16-position spin-labeled phosphatidylcholines at higher temperatures

To investigate the effects of the polymer-lipids with different polar-headgroup sizes on the rotational dynamics of the DPPC/PEG-DPPE dispersions in the fluid phase, ESR measurements with 5- and 16-PCSL were also carried out at 50°C. Plots of the difference between the outer and the inner hyperfine splittings, $\Delta A = 2(A_{max} - A_{min})$, for 5-PCSL and of the apparent linewidth of the high-field hyperfine manifold, ΔH, for 16-PCSL are given as a function of the lipid composition for the three different polymer-lipids in Fig. 5. Unlike the situation at 10°C, where the lamellar component
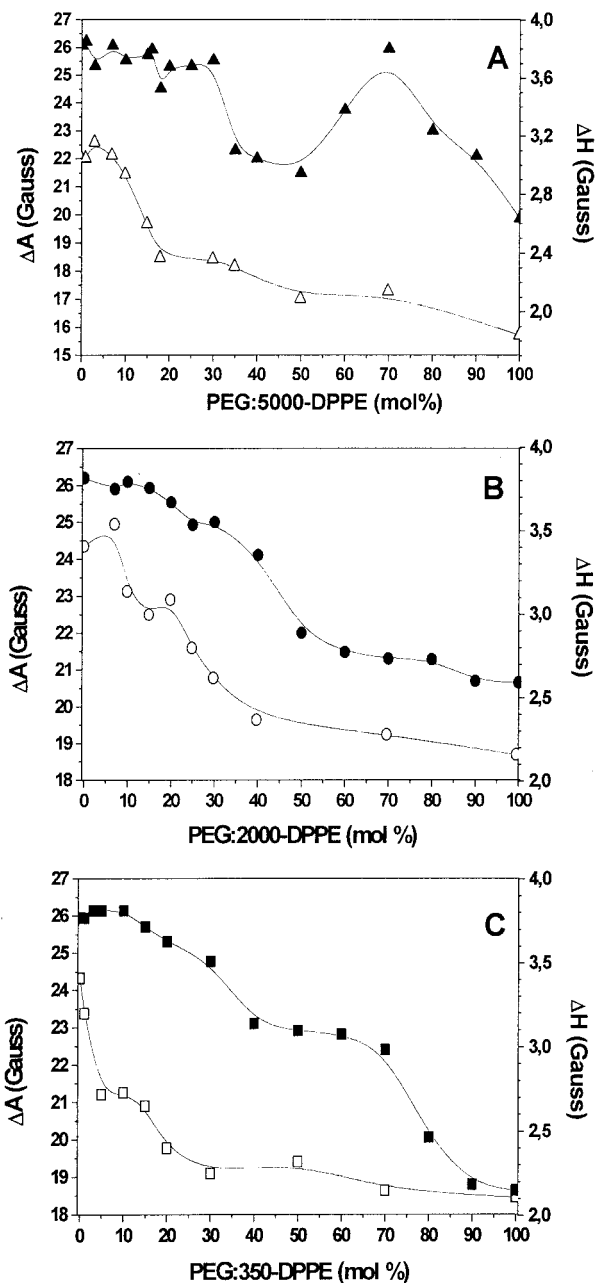

FIGURE 5 Dependence of the difference between the outer and the inner hyperfine splittings, ΔA, of the 5-PCSL spin label (*solid symbols*) and of the width, ΔH, of the high-field hyperfine line of the 16-PCSL spin label (*open symbols*) on PEG-DPPE lipid content in aqueous dispersions of (*A*) DPPC/PEG:5000-DPPE mixtures at 50°C, (*B*) DPPC/PEG:2000-DPPE mixtures at 50°C, and (*C*) DPPC/PEG:350-DPPE mixtures at 45°C. The errors are smaller than the symbols.

of the mixed lipid dispersion is in the gel phase, two spectral components are not resolved for any polymer-lipid content at 50°C. All spectra of 5-PCSL are essentially single-component, axially averaged anisotropic powder patterns, and all spectra of 16-PCSL approximate to single, isotropic, differentially broadened ^{14}N hyperfine triplets (cf. Belsito et

al., 2000). Separate spectral components corresponding to the lamellar and micellar phases are not resolved in the fluid state. The ESR spectra observed in the coexistence region therefore reflect a composite of both bilayer and micelle structures. In general, however, there is a trend toward increasing lipid chain mobility with increasing content of PEG-lipid. This reflects, in a rather global way, the more highly dynamic environment of the lipid chains in the hydrophobic core of the polymer lipid micelles than that in lamellar structures. Interestingly, the values of ΔA change first only relatively slowly with increasing content of polymer lipid for all three PEG chainlengths. Although the explanation for this is not entirely certain, it implies that the difference between the chain mobilities in the lamellar and micellar states is not very different at low contents of polymer lipid, especially for those of longer chainlength. The most interesting and significant feature of Fig. 5, however, is that for PEG:5000-DPPE mixtures the "anomalous" increase in $2A_{max}$ observed at 10°C with 5-PCSL (Fig. 3 A) is reproduced in the dependence of ΔA on PEG-lipid content in the fluid phase at 50°C. In addition, the dependence of ΔA on concentration of bulk free PEG:5000 in the suspending medium of DPPC/PEG:5000-DPPE dispersions (data not shown) parallels that of $2A_{max}$ given in Fig. 3 A, inset.

DISCUSSION

Spectrophotometry

Compared with previous turbidity measurements on DPPC mixtures with PEG-lipids bearing short polymer headgroups (Belsito et al., 2000), the results in Fig. 1 show that the PEG:5000-DPPE polymer lipid is more effective in disaggregating the multilamellar lipid vesicles than is PEG:350-DPPE. However, in the micellar region up to 40 mol % PEG:5000-DPPE, the optical densities are appreciably higher than those of DPPC mixtures with either PEG:2000-DPPE or PEG:350-DPPE when these are wholly in the micellar phase. This suggests a different micellar structure for mixtures with the long PEG:5000-DPPE polymer lipid in the intermediate composition range. To a certain extent, this difference is also mirrored in the 5-PCSL values of $2A_{max}$ in the micellar regime (see Fig. 3). Additionally, the difference in optical density between low and high temperatures (viz., 10 and 50°C) persists in the micellar regime up to 70 mol % PEG:5000-DPPE, unlike the situation for mixed micelles containing the shorter polymer lipids (cf. Belsito et al., 2000). Apparently, the micelles in this regime are still capable of undergoing an attenuated chain-melting transition (see Fig. 1). This might indicate that the micelles in this regime consist of bilayer fragments or plates that are solubilized by PEG-lipid, somewhat as found for mixed micelles of PC with cholate (Small, 1986). Significantly, the upper boundary at 70 mol % PEG:5000-DPPE corresponds to the local maximum in both $2A_{max}$ and ΔA for 5-PCSL—

and the region between 40 and 70 mol % PEG:5000 DPPE to that of their "anomalous" behavior—in these mixtures (cf. Figs. 3 A and 5 A) that is discussed later. In making these comparisons it has to be borne in mind that several different factors, such as particle size, number of particles, and polydispersity, as well as refractive index, contribute to the turbidity of the lipid dispersions.

Lipid packing density

As already stated in the Results section, the dependence of $2A_{max}$ for 5-PCSL on polymer lipid content (see Fig. 3) directly reflects the expansion in surface area that is induced by the lateral pressure in the polymer brush. Such an expansion is expected from the known behavior of surface-grafted polymers (see, e.g., De Gennes, 1979) and consideration of the effects of lateral pressure in lipid membranes (see, e.g., Marsh, 1996). It may be understood semi-quantitatively by a combination of models from polymer physics with the equation of state for lipid monolayers and bilayers.

The variation in lateral lipid packing density with content of polymer-lipid is obtained by an extension of the treatment of the interfacial equilibrium in lipid membranes that was given by Israelachvili and co-workers (see, e.g., Israelachvili et al., 1980; Cevc and Marsh, 1987). The interfacial free energy of a lipid molecule in a lyotropic aggregate is given by:

$$\Delta F_{int} = \gamma A_l + C_o/A_l + \Delta F_{rep}^{brush} \qquad (4)$$

where the first two terms represent the bare interaction of the lipids with water and between lipids, respectively, in the absence of polymer headgroups. Here γ is the cohesive hydrophobic free energy density, A_l is the area per lipid molecule at the polar-apolar interface, and C_o is a constant characterizing the repulsive interactions between lipids. The final term in Eq. 4 represents the repulsive interactions between polymer headgroups in the brush regime. In the mean-field theory used previously by Hristova and Needham (1994, 1995) for polymer lipids, this term is related to the polymer grafting density by Milner et al. (1988):

$$\Delta F_{rep}^{brush} \approx k_B T n_p a_m^{4/3} (X_{PEG}/A_l)^{2/3} \times X_{PEG} \qquad (5)$$

where n_p is the degree of polymerization, a_m is the size of a monomer unit, and X_{PEG} is the mole fraction of polymer lipid. The additional factor of X_{PEG} in Eq. 5 is to give the free energy per lipid, rather than per polymer. An expression identical to Eq. 5 holds also in the De Gennes scaling theory, except that the exponents 2/3 and 4/3 are replaced by 5/6 and 5/3, respectively (Alexander, 1977).

Minimizing the free energy in Eq. 4 with respect to the lipid area, A_l (or with respect to the area per polymer) then gives rise to the following expression for the equilibrium

area per lipid molecule:

$$A_l^2 = A_{l,o}^2 + \frac{2}{3} \frac{k_B T}{\gamma} n_p a_m^{4/3} X_{PEG}^{5/3} A_l^{1/3} \tag{6}$$

where $A_{l,o} = (C_o/\gamma)^{1/2}$ is the equilibrium area per lipid molecule in the absence of the polymer brush. For PEG:5000-DPPE (i.e., $n_p = 114$) admixed at a mole fraction of $X_{PEG} = 0.03$ in DPPC at 10°C, an ~1% increase in surface area is predicted from Eq. 6 with $a_m = 0.39$ nm (Evans et al., 1996), $A_{l,o} = 0.49$ nm^2 (Marsh, 1990), and $\gamma = 35 \times 10^{-21}$ J/nm^2 (Cevc and Marsh, 1987). Assuming a typical value for the area thermal expansion coefficient of 0.001 K^{-1} at 10°C (see, e.g., Marsh, 1996), this increase in membrane area would be produced by an increase in temperature of ~10°. Experimentally, a temperature increase of this size produces a decrease in $2A_{max}$ of ~1.5 G with 5-PCSL in gel-phase DPPC. This is equal to the change in $2A_{max}$ induced by 3 mol % of PEG:5000-DPPE in DPPC at 10°C (Fig. 3 A). The agreement of the theoretical predictions with experiment is therefore rather satisfactory. Increases in membrane area for admixture of the shorter polymer lipids, PEG:2000-DPPE ($n_p = 45$) and PEG:350-DPPE ($n_p = 8$), are also predicted to be in the region of 1–2%, at the mole fractions corresponding to the onset of micelle formation, as for PEG:5000-DPPE. Scaling theory also gives predictions similar to those of mean-field theory at these levels of polymer lipid.

It should be noted that calculations of this type, with the standard value for the hydrophobic free energy density γ, reliably reproduce the elastic modulus for area extension, K_A, of fluid lipid bilayers. Consequently, they may overestimate (by a factor given by the inverse ratio of the K_A values) the area expansion produced in gel-phase bilayers. This does not, however, affect the validity of the comparison with the decrease in A_{max} produced by increase in temperature, also in the gel phase. Evans and Waugh (1977) have demonstrated that the thermal expansion coefficient also scales as $1/K_A$, and therefore the two effects cancel in the comparison given above.

Effects of high PEG:5000-DPPE contents

A possible explanation for the increase in $2A_{max}$ and ΔA of 5-PCSL at polymer-lipid contents over the range 50–70 mol % for the long PEG:5000 polymer headgroup (see Figs. 3 A and 5 A) was referred to already in the Results section. This involved the effects on lipid packing density of partial dehydration of the lipid surface by the high-molecular-weight grafted polymer. An alternative, or additional, explanation is based on the enhanced tendency of the long polymer to induce membrane curvature. This latter mechanism can be analyzed by using the methods introduced in the previous section.

A grafted polymer favors surface curvature, i.e., micelle formation, because the center of action of the polymer lateral pressure is offset from the polar-apolar interface at which A_l is defined in Eq. 4. (The sign of this curvature is that appropriate to normal, rather than inverted, micelles.) We assume, as a reasonable approximation, that the polymer headgroup interactions are centered at a distance $L/2$ from the polar-apolar interface, where L is the equilibrium extension of the polymer brush. The latter is given by Hristova and Needham (1994) and Alexander (1977):

$$L \approx n_p a_m^{5/3} (X_{PEG}/A_l)^{1/3} \tag{7}$$

which is valid for both mean-field and scaling theories.

For a curved lipid aggregate, the area per lipid molecule, A_l', at height $L/2$ from the polar-apolar interface is that which should appear in Eq. 5 for the free energy of the polymer brush. In a cylindrical micelle, for example, the two areas are related by simple geometry:

$$A_l' = A_l(1 + L/2R) \tag{8}$$

where R is the radius of the micelle at the polar-apolar interface. The latter depends on the aggregation number of the micelle that is given by:

$$n_{agg} = 2\pi R h / A_l \tag{9}$$

where h is the length of the cylindrical micelle. Combining Eqs. 5 and 7–9 then leads to the following expression for the repulsive free energy of the polymer brush:

$$\Delta F_{rep}^{brush} \approx \frac{C_1}{A_l^{2/3}(1 + c_2/A_l^{4/3})^{2/3}} \tag{10}$$

where

$$C_1 \approx k_B T n_p a_m^{4/3} X_{PEG}^{5/3}$$

and

$$c_2 \approx (\pi h/n_{agg}) n_p a_m^{5/3} X_{PEG}^{1/3}.$$

Minimizing the corresponding total free energy in Eq. 4 with respect to the lipid area, A_l, gives the following first-order approximation for the dependence of the change in lipid packing density on content of polymer-lipid in a cylindrical micelle:

$$A_{l,o} - A_l \approx -a_1 n_p X_{PEG}^{5/3} (1 - \tfrac{1}{3} a_2 n_p X_{PEG}^{1/3})/(1 + a_2 n_p X_{PEG}^{1/3})^{5/3} \tag{11}$$

where the numerical scaling constants are given by $a_1 \approx (1/3)(k_B T/\gamma)(a_m^2/A_{l,o})^{2/3}$ and $a_2 \approx (\pi h/n_{agg})a_m^{5/3}/A_{l,o}^{4/3}$. This function first decreases with increasing values of X_{PEG}, reaches a minimum, and then increases continuously beyond the single minimum. Qualitatively similar predictions are obtained from equivalent calculations for spherical micelles. The numerical scaling, however, is understandably

different. Qualitatively similar results are also obtained by using scaling theory, instead of mean-field theory, for Eq. 5.

The dependence of the lipid packing density on mole fraction of polymer lipid that is predicted by Eq. 11 is shown in Fig. 6. Curves are compared for three different degrees of polymerization, n_p = 8, 45, and 114, that correspond to PEG:350, PEG:2000, and PEG:5000, respectively. Because of uncertainties in the structural parameters of the micelles, the scaling of the x axis has been chosen empirically to locate the minimum for PEG:5000 DPPE at a mole fraction of 0.5. This facilitates the comparison with experiment. Of principle interest is the dependence on degree of polymerization that is given explicitly by the model. Whereas the packing density decreases to a minimum and then increases with increasing content of PEG:5000 polymer lipid, that for admixtures of the shorter polymer lipids PEG:2000 and PEG:350 decreases continuously over the range of polymer lipid contents shown.

These predictions for the lipid packing density parallel the relative dependencies of the outer hyperfine splittings $2A_{max}$ and hyperfine anisotropies ΔA of 5-PCSL, in the micellar regions of Figs. 3 and 5, respectively. Therefore, the model given in Fig. 6 provides an additional possible rationale for the rather different behavior of spin-labeled phosphatidylcholine in micelles containing the high-molecular-weight PEG:5000 lipid, as compared with the lower-molecular-weight PEG:2000 and PEG:350 lipids. The long polymer is more effective in reducing the lipid packing de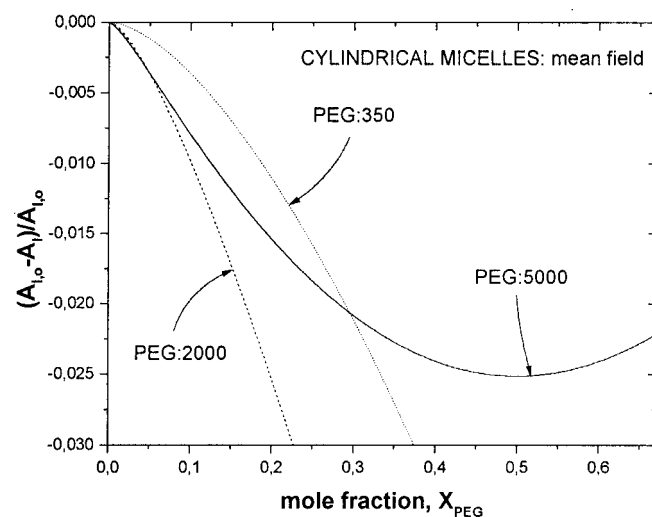nsity at low concentrations (see Fig. 6). However, the polymer brush extends further from the polar-apolar interface for PEG:5000 than for PEG:2000 or PEG:350. The result of this is that the minimum in packing density is achieved more readily for the PEG:5000 lipid. The splay of the polymers at the periphery of the brush region evidently then requires an increase in packing density at the polar-apolar interface.

A feature of the results in Figs. 3 and 5 that is not explained directly by this simple model is the final decrease in $2A_{max}$ and ΔA at very high contents of the PEG:5000 lipid. Beyond the minimum, the packing density is predicted by Eq. 11 to increase continuously with increasing content of PEG:5000 lipid. Departures from the predicted behavior would occur if the structure of the mixed micelles changes at contents of PEG:5000 lipid >70 mol %. Theoretical predictions by Hristova and Needham (1995) place the transition between cylindrical and spherical micelles at much lower contents of PEG:5000 lipid. Cryoelectron microscopy reveals the coexistence of thread-like and globular micelles when 40 mol % of PEG:2000 lipid is mixed with egg phosphatidylcholine (Edwards et al., 1997). This also suggests that a transition between cylindrical and spherical micelles occurs at concentrations <70 mol % for PEG:5000 lipids. Any change in micellar structure at 70 mol % PEG:5000 lipid is therefore other than that from cylinders to spheres.

Lamellar-micellar transition

On the whole, the results on lamellar-micellar coexistence presented in Fig. 4 are reasonably consistent with two previous determinations using PEG-lipids of different fatty acid chain composition and, in one case, different non-polymer lipid host (Baekmark et al., 1997; Rex et al., 1998). The main difference is that values of X_{PEG}^{end} obtained by indirect calorimetric methods (Baekmark et al., 1997) are approximately half those found here. Observation of micelle formation as a distinct spectral component, as is done here, is a rather more direct approach.

The systematic data that we have obtained by using a consistent experimental protocol allows consideration of the scaling with polymer chainlength. Hristova and Needham (1994) have estimated the saturation values of polymer lipid that can be incorporated in the lamellar phase by equating the lateral pressure in the polymer brush with the maximum tension that a bilayer vesicle can support. An equivalent treatment was also given by the same authors in terms of the maximum area extension of the vesicle membrane (Hristova and Needham, 1995). These saturation values are higher than the polymer lipid content, X_{PEG}^{on}, at the onset of the bilayer-to-micelle transition (Hristova and Needham, 1995). Although this implies that the bilayer-micelle transition takes place at a lower polymer pressure than the maximum tensile strength of the bilayer, the scaling with polymer chain length may still be similar.

FIGURE 6 Decrease, $A_{l,o} - A_l$, in area per lipid molecule at the polar-apolar interface as a function of mole fraction, X_{PEG}, of polymer lipid in cylindrical micelles. Calculations are from Eq. 11, with n_p = 8, 45, and 114, corresponding to PEG:350, PEG:2000, and PEG:5000 lipids, respectively. The value of a_2 is chosen to locate the minimum for PEG:5000 lipid at X_{PEG} = 0.5. The value of a_1 is calculated with a_m = 0.39 nm, $A_{l,o}$ = 0.6 nm^2, γ = 35 $\times$ 10^{-21} J/nm^{-2}, and T = 293 K. Qualitatively similar dependences are obtained from calculations for spherical micelles.

The area expansion induced by the polymer brush in the lamellar phase is given by Eq. 6. Let us assume that the onset of micellization takes place at some fixed critical area expansion, $A_l^{crit} - A_{l,o}$, which is lower than the maximum increase in area that a bilayer vesicle can support. This is justified by the fact that the onset of micellization occurs at approximately the same value of A_{max} for 5-PCSL (i.e., at the same lipid packing density) in the lamellar phase for all three PEG-lipids (see Fig. 3). Then it is seen immediately from Eq. 6 that the dependence of X_{PEG}^{on} on polymer chain length is given by $X_{PEG}^{on} \sim n_p^{-3/5}$. This is the result from mean-field theory. From scaling theory, the corresponding exponent of n_p is $-6/11$ (Hristova and Needham, 1994). The experimental data in Fig. 4 give a scaling of X_{PEG}^{on} with n_p that has an exponent of -0.74 ± 0.06. This exponent is similar to the theoretical predictions and closer to that from mean-field theory, although it is still somewhat greater than the latter.

In contrast, the experimental values of X_{PEG}^{end} that characterize the completion of the lamellar-micellar transition have a considerably weaker dependence on polymer chain-length than does X_{PEG}^{on} (see Fig. 4). The values of X_{PEG}^{end} are characterized by an effective exponent of n_p that is -0.33 ± 0.04. It is to be expected that X_{PEG}^{end} depends more strongly on the properties of the micelles than does X_{PEG}^{on}. An interpretation may be given in terms of Eqs. 6 and 11 for the area expansion in the coexisting lamellar and micellar phases. From the phase rule, the compositions of the lamellar and micellar phases remain constant at values of X_{PEG}^{on} and X_{PEG}^{end}, respectively, throughout the transition. Therefore, the areas per lipid molecule will remain constant with values of A_l^{bil} and A_l^{mic} for the bilayers and micelles, respectively. Combining the first-order approximation of Eq. 6 for bilayers with Eq. 11 for micelles then gives the ratio of polymer lipid compositions at the onset and completion of the transition as:

$$X_{PEG}^{on}/X_{PEG}^{end} \approx \left(\frac{\Delta A_l^{bil}}{\Delta A_l^{mic}}\right)^{3/5} \left(\frac{A_l^{bil}}{A_l^{mic}}\right)^{2/5} \frac{[1 - 1/3a_2n_p(X_{PEG}^{end})^{1/3}]^{3/5}}{[1 + a_2n_p(X_{PEG}^{end})^{1/3}]} \quad (12)$$

where ΔA_l^{mic} and ΔA_l^{bil} are the expansions in area per lipid molecule by the polymer brush in the micellar and bilayer phases, respectively. This equation predicts that the ratio $X_{PEG}^{on}/X_{PEG}^{end}$ should decrease with increasing polymer chainlength, n_p, but with a steadily decreasing slope. The data from Fig. 4 are plotted according to Eq. 12 in Fig. 7. It is seen that Eq. 12 provides a reasonable description of the dependence on polymer chainlength. The effect of the multiplying factors $(X_{PEG}^{end})^{1/3}$ on the right-hand side of Eq. 12 is relatively minor. The dependence shown in Fig. 7 is dominated by n_p. A comparably good fit to that given in Fig. 7 is also obtained with the corresponding expression derived from scaling theory. The fitted value of $(\Delta A_l^{bil}/\Delta A_l^{mic})^{3/5}$ $(A_l^{bil}/A_l^{mic})^{2/5}$ is ~0.36, which is at least qualitatively in
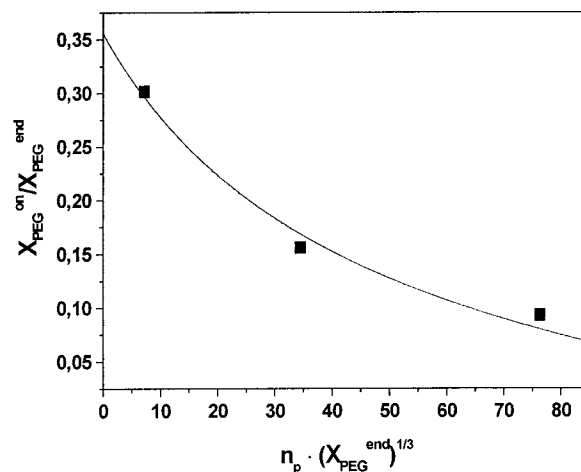

FIGURE 7   Dependence of the ratio, $X_{PEG}^{on}/X_{PEG}^{end}$, of polymer lipid composition at the onset and completion of the bilayer to micelle transition, in mixtures of PEG-DPPE with DPPC, on the scaled polymer chainlength, n_p $(X_{PEG}^{end})^{1/3}$. Data points (*squares*) are obtained from Fig. 4. The solid line represents a nonlinear least-squares fit with Eq. 12 (mean-field theory), where $(\Delta A_l^{bil}/\Delta A_l^{mic})^{3/5} \times (A_l^{bil}/A_l^{mic})^{2/5}$ *and* a_2 are adjustable fitting parameters. The dashed line is the corresponding fit with scaling theory.

agreement with the expectation that the area/lipid molecule is considerably greater in the micelles than in the lamellar phase.

CONCLUSIONS

Lipid spin-label ESR was used to investigate the influence of polymer-lipid headgroup size on both the lipid packing density and micelle formation in dispersions with phosphatidylcholine: 1) the onset of micelle formation by PEG-lipids in mixed lipid dispersions occurs at a fixed lipid packing density, already in the gel phase; 2) the mole fraction of polymer lipid at the onset of micelle formation scales with an exponent of the polymer headgroup size near to that predicted theoretically; 3) the mole fraction of PEG-lipid at the completion of micelle formation is a weaker function of polymer headgroup size, which again is consistent with theoretical predictions; 4) the behavior of PEG: 5000-DPPE at high mole fractions differs qualitatively from that of shorter polymer lipids. This could have generic implications for the design of sterically stabilized liposomes. Although only latent at the lower polymer lipid contents necessarily used in liposomal delivery systems, such differences may, for example, be reflected in the release process.

REFERENCES

Alexander, S. 1977. Adsorption of chain molecules with a polar head. A scaling description. *J. de Physique.* 38:983–987.

Allen, T. M., C. Hansen, F. Martin, C. Redemann, and A. Yau-Yong. 1991. Liposomes containing synthetic lipid derivatives of poly(ethylene glycol) show prolonged circulation half-lives in vivo. *Biochim. Biophys. Acta.* 1066:29–36.

Baekmark, T. R., S. Pedersen, K. Jørgensen, and O. G. Mouritsen. 1997. The effects of ethylene oxide-containing lipopolymers and tri-block copolymers on lipid bilayers of dipalmitoylphosphatidylcholine. *Biophys. J.* 73:1479–1491.

Bartucci, R., T. Páli, and D. Marsh. 1993. Lipid chain motion in an interdigitated gel phase: conventional and saturation transfer ESR of spin-labelled lipids in dipalmitoylphosphatidylcholine-glycerol dispersions. *Biochemistry.* 32:274–281.

Belsito, S., R. Bartucci, G. Montesano, D. Marsh, and L. Sportelli. 2000. Molecular and mesoscopic properties of hydrophilic polymer-grafted phospholipids mixed with phosphatidylcholine in aqueous dispersion: interaction of dipalmitoyl *N*-poly(ethylene glycol)phosphatidylethanolamine studied by spectrophotometry and spin-label electron spin resonance. *Biophys. J.* 78:1420–1430.

Blume, G., and G. Cevc. 1990. Liposomes for the sustained drug release in vivo. *Biochim. Biophys. Acta.* 1029:91–97.

Blume, G., and G. Cevc. 1993. Molecular mechanism of the lipid vesicles longevity in vivo. *Biochim. Biophys. Acta.* 1146:157–168.

Cevc, G., and D. Marsh. 1987. Phospholipid Bilayers. Physical Principles and Models. Wiley-Interscience, New York.

De Gennes, P. G. 1979. Scaling Concepts in Polymer Physics. Cornell University Press, London.

Edwards, K., M. Johnsson, G. Karlsson, and M. Silvander. 1997. Effect of polyethyleneglycol-phospholipids on aggregate structure in preparations of small unilamellar liposomes. *Biophys. J.* 73:258–266.

Evans, E., D. J. Klingenberg, W. Rawicz, and F. Szoka. 1996. Interactions between polymer-grafted membranes in concentrated solutions of free polymer. *Langmuir.* 12:3031–3037.

Evans, E. A., and R. Waugh. 1977. Mechano-chemistry of closed, vesicular membrane systems. *J. Colloid Interface Sci.* 60:286–298.

Hristova, K., and D. Needham. 1994. The influence of polymer-grafted lipids on the physical properties of lipid bilayers: a theoretical study. *J. Colloid Interface Sci.* 168:302–314.

Hristova, K., and D. Needham. 1995. Phase behavior of a lipid/polymer-lipid mixture in aqueous medium. *Macromolecules.* 28:991–1002.

Israelachvili, J. N., S. Marcelja, and R. G. Horn. 1980. Physical principles of membrane organization. *Q. Rev. Biophys.* 13:121–200.

Klibanov, A. L., K. Maruyama, V. P. Torchilin, and L. Huang. 1990. Amphipathic polyethylene glycols effectively prolong the circulation time of liposomes. *FEBS Lett.* 268:235–237.

Lasic, D. D. 1993. Liposomes: From Physics to Applications. Elsevier, Amsterdam-London-New York.

Lasic, D. D., and F. Martin. 1995. Stealth Liposomes. CRC Press, Boca Raton, London, Tokyo.

Lasic, D. D., F. J. Martin, A. Gabizon, S. K. Huang, and D. Papahadjopoulos. 1991. Sterically stabilized liposomes: a hypothesis on the molecular origin of the extended circulation times. *Biochim. Biophys. Acta.* 1070:187–192.

Lasic, D. D., and D. Needham. 1995. The "stealth" liposome: a prototypical biomaterial. *Chem. Rev.* 95:2601–2628.

Mabrey, S., and J. M. Sturtevant. 1976. Investigation of phase transitions of lipids and lipid mixtures by high sensitivity differential scanning calorimetry. *Proc. Natl. Acad. Sci. USA.* 73:3862–3866.

Marsh, D. 1981. Electron spin resonance: spin labels. *In* Membrane Spectroscopy. Molecular Biology, Biochemistry and Biophysics, Vol. 31. E. Grell, editor. Springer-Verlag, Berlin, Heidelberg, New York. 51–142.

Marsh, D. 1982. Electron spin resonance: spin label probes. *In* Techniques in Lipid and Membrane Biochemistry, Vol. B4/II. J. C. Metcalfe and T. R. Hesketh, editors. Elsevier, Amsterdam. B426–1–B426/44.

Marsh, D. 1989. Experimental methods in spin-label spectral analysis. *In* Biological Magnetic Resonance, Vol. 8. L. J. Berliner and J. Reuben, editors. Plenum Publishing Corp., New York. 255–303.

Marsh, D. 1990. Handbook of Lipid Bilayers. CRC Press, Boca Raton, FL.

Marsh, D. 1996. Lateral pressure in membranes. *Biochim. Biophys. Acta.* 1286:183–223.

Milner, S. T., T. A. Witten, and M. E. Cates. 1988. A parabolic density profile for grafted polymers. *Europhys. Lett.* 5:413–418.

Papahadjopoulos, D., T. M. Allen, A. Gabizon, E. Mayhew, K. Matthay, S. K. Huang, K.-D. Lee, M. C. Woodle, D. D. Lasic, C. Redemann, and F. J. Martin. 1991. Sterically stabilized liposomes. Improvements in pharmacokinetics and antitumor therapeutic efficacy. *Proc. Natl. Acad. Sci. USA.* 88:11460–11464.

Rex, S., M. J. Zuckermann, M. Lafleur, and J. R. Silvius. 1998. Experimental and Monte Carlo simulation studies of the thermodynamics of polyethyleneglycol chains grafted to lipid bilayers. *Biophys. J.* 75:2900–2914.

Small, D. M. 1986. The physical chemistry of lipids: from alkanes to phospholipids. *In* Handbook of Lipid Research, Vol. 4. D. M. Small, editor. Plenum Press, New York, London. 70–72.

Tirosh, O., Y. Barenholz, J. Katzhendler, and A. Priev. 1998. Hydration of polyethylene glycol-grafted liposomes. *Biophys. J.* 74:1371–1379.

Torchilin, V. P., V. P. Omelyanenko, M. I. Papisov, Jr., A. A. Bogdanov, V. S. Trubetskoy, J. N. Herron, and C. A. Gentry. 1994. Poly(ethylene glycol) on the liposome surface: on the mechanism of polymer-coated liposome longevity. *Biochim. Biophys. Acta.* 1195:11–20.